Journal of Flow Visualization & Image Processing, vol. 5, pp. 95-103, 1998

INSTANTANEOUS AND PLANAR VISUALIZATION OF SUPERSONIC GAS JETS AND SPRAYS

T. K. Kim, S. Y. Son, and K D. Kihm
Department of Mechanical Engineering, Texas A&M University, College Station, TX 77843-3123

An alternative use of Rayleigh- and Mie-scattering techniques allows separate examination of high-speed air jets and their airblast atomization characteristics. The molecular clusters of condensed vapor in sonic or supersonic gas jets fall in the Rayleigh range ($d \ll \lambda$) and *the scattered light from these particles can visualize the development of high-speed jets and shear mixing with ambient air. When the tested liquid is injected, the Mie-scattering signals from the spray droplets, which are in the Mie range* ($d = \lambda$ *or* $d \geq \lambda$), *enable visualization of the liquid spray development. A comparative study of gas jets and sprays has been made for both converging nozzle (SN type) and a converging-diverging nozzle (CD type). The present visualization study reveals some explanations for the different atomization characteristics of the two types of nozzles under identical injection conditions.*

INTRODUCTION

Compressed gas accelerates when it exhausts through a converging or convergingdiverging nozzle. Once the converging nozzle (SN type) is choked with a unit exit Mach number, the underexpanded sonic jet establishes the Prandtl-Meyer expansion fans at the nozzle exit (Fig. la). However, the converging-diverging nozzle (CD type) under the same stagnation pressure develops an overexpanded supersonic jet and the oblique shocks, followed by the expansion fans, are established at the nozzle exit (Fig. lb). This nearly opposite nature of the initial development of the two jets may alter their airblast interactions with the injected liquid, spray angles, and atomization characteristics.

Several previous studies [1,2,3] have investigated the atomization characteristics of different injected materials under various levels of high-speed gas jets. The recent work of Park et al. [4] presents a comparative study of airblast atomization under underexpanded sonic and overexpanded supersonic gas jets. They have presented experimentally extrapolated spray Sauter mean diameter *(SMD)* for the two types of nozzles (SN and CD types) using the line-of-sight Malvern measurement technique. Tomographic reconstruction of the Malvern data and a Buckingham-PI dimensional analysis of the reconstructed data have provided a single experimental correlation for both nozzles as:

$$\frac{SMD}{d_o} = A\left(\frac{x}{d_o}\right)^{-0.1367}\left(\frac{r}{d_o}\right)^{0.3742}\left(\frac{\dot{m}_L''}{\sqrt{\rho_L p_b}}\right)^{0.3588}\left(\frac{p_t}{p_b}\right)^{-0.7801} \tag{1}$$

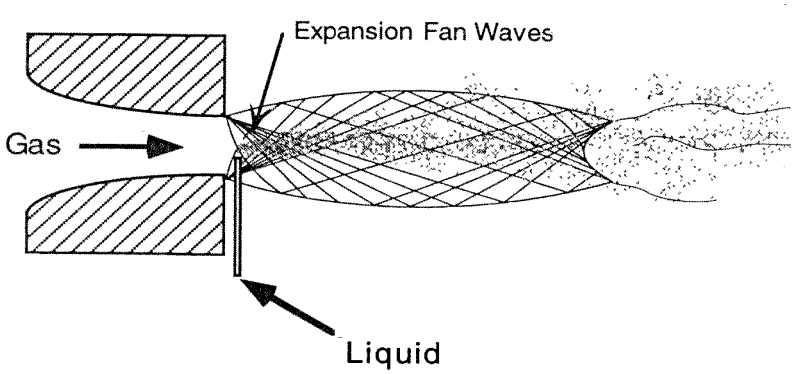

(a) Underexpanded Sonic Jet from he SN-type Nozzle.

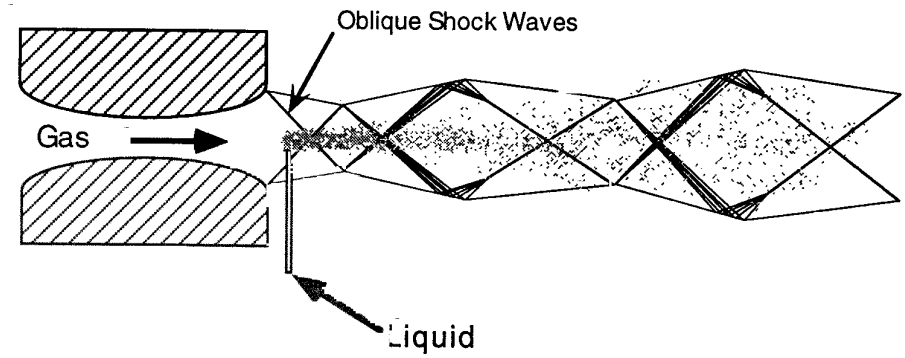

(b) Overexpanded Supersonic Jet from the CD-type Nozzle

Fig. 1 Development of high-speed gas jets,

where x and r represent the axial and radial coordinates, respectively, d_o denotes the liquid orifice diameter, $\dot{m}_L$ is the injected liquid flux of density ρ_L, and the subscripts t and b refer to total (or stagnation) pressure and back pressure, respectively.

The geometric constant A was determined as $A = 0.0329$ for the SN type nozzle, and $A = 0.0355$ for the CD type nozzle. The SN type jet provides slightly better atomization than the CD type nozzle despite the fact that the latter develops a jet with a higher Mach number than the former. It is conjectured that the primary reason for the difference in their atomization efficiencies is the largely different initiation of atomization with either shock waves or expansion waves, as illustrated in Fig. 1. This difference can alter the spray angle and divergence, thereby altering the droplet coalescence and their *SMD*s.

Although it seems necessary to interpret some significant dependence of the atomization characteristics on the interaction of the gas jet with atomized liquid, few attempts have been made to visualize the spray and gas jet development. The present work visualizes the gas jets and liquid sprays alternatively using Rayleigh- and Mie-scattering techniques, and a comparison has been made to examine the differences of underexpanded sonic and overexpanded supersonic gas

EXPERIMENT

When gas accelerates through either a converging nozzle or a converging-diverging nozzle, the gas temperature near the nozzle exit significantly drops due to the conversion of the internal or molecular thermal energy into the macroscopic or kinetic flow energy during the isentropic expansion. This low-temperature gas quickly condenses its naturally contained water vapor molecules (about 0.1 nm in size) into relatively larger clusters (approximately 10 nm in size). These molecular clusters are in the range of Rayleighscattering [5], i.e., $d \ll \lambda$, and can be used as natural seeding in visualizing the high-speed gas jets in the absence of atomized liquid. The condensed vapor clusters make excellent tracers, with virtually no slip from the gas flow because of their small size and negligible inertia [6].

When a small spherical particle $(d \ll \lambda)$ is illuminated by a vertically polarized laser sheet (Fig. 2), the Rayleigh-scattered light [7] also carries only a vertically polarized component, with respect to the viewing direction. Therefore, the Rayleigh image is fully recorded when the polarizer filter is aligned vertically, and the image should disappear when the filter is aligned horizontally. The Rayleigh scattering intensity is proportional to

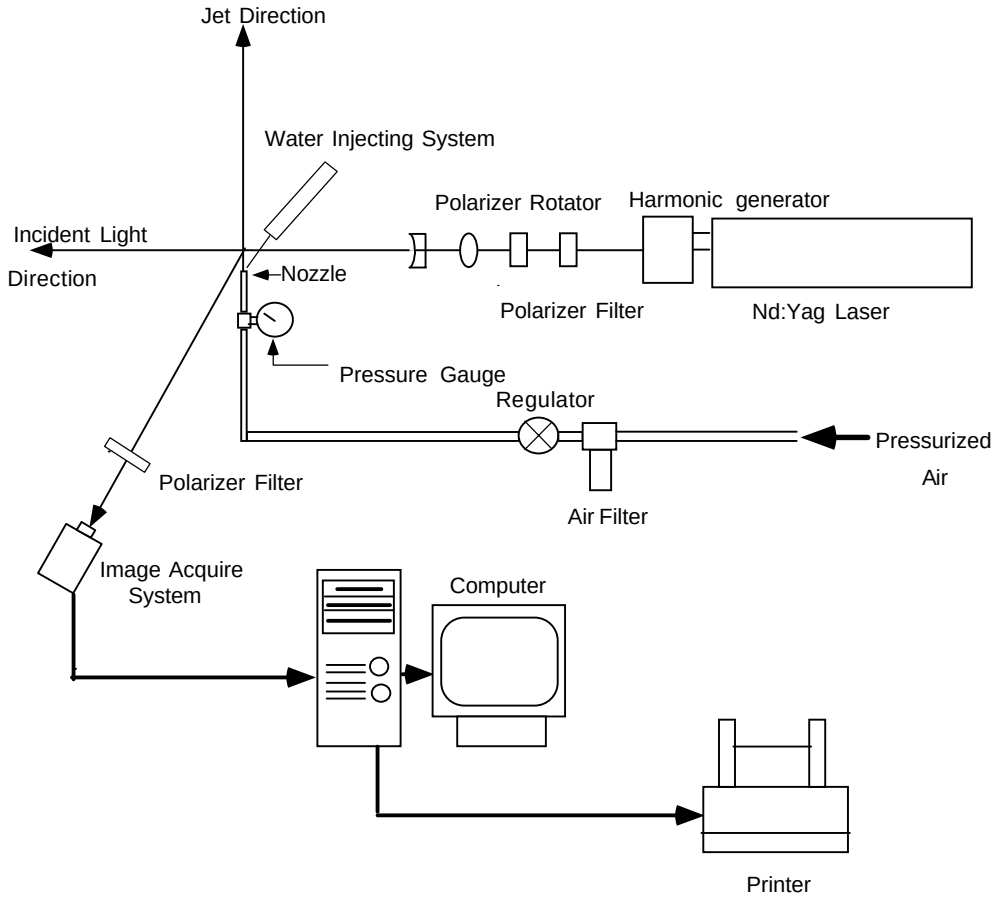

Fig. 2 A schematic diagram of overall experimental apparatus.

the incident beam intensity I_o and increases inversely with its wavelength by an exponent of 4, i.e., $(1/\lambda)^4$. More description and detailed derivations of the Rayleigh scattering phenomena are summarized in the Master's thesis by Kim [8].

The present experiment uses a pulsed Nd:YAG laser that generates visible green light (λ = 532 nm) in the second harmonic mode of more than 100 mJ per pulse. The Q-switched mode allows an ultrashort pulse of approximately 7 ns so that an extremely short temporal resolution records frozen images of high-speed gas jets and sprays. A series of concave, convex, and cylindrical lenses collimates and expands the laser beam of about 8 mm diameter into a thin sheet of about 0.2 mm thickness minimum. The thin laser sheet tomographically visualizes the gas jets and sprays. The linear polarizer filter located in front of the image-acquiring system (either 35 mm or CCD camera) acts to gate the Rayleigh scattering signal that is fully recorded only when the polarizer filter is vertically oriented. The CCD images are stored on videotape first and are then digitized directly by an Apple Macintosh Centris computer with an A/V card with the aid of Adobe Photoshop. Finally, hard copies can be printed by means of a laser printer.

When the tested liquid is injected, the gas jet shatters the liquid and develops airblast sprays. Most liquid spray drops are in the Mie scattering range [9], i.e., $d = \lambda$ or $d \geq \lambda$, and the spray development can be readily visualized by recording the scattering images from the spray drops. The scattered light intensity is a strong function of the spherical observation angle, and the angular dependence of the intensity is also a function of the particle diameter. The Mie scattering intensity is several orders of magnitude higher than the Rayleigh scattering for a given incident beam. The same experimental setup as seen in Fig. 2 allows the recording of Mie scattering images.

RESULTS AND DISCUSSION

The visualization experiment has been performed for subsonic, sonic, and supersonic gas jets for both the SN type and CD type nozzles. For the spray visualization, in addition to the stagnation pressure variation, the injected liquid flow rate has also been varied to range different air-to-liquid ratios (ALR). Digitized images of the recordings have been analyzed to identify the overall spray development depending on the jet Mach number.

Jet Mixing and Development

Figure 3 shows a series of digitally recorded images of air jets exhausted from the SN type nozzle with 6.07 mm^2 exit area at different stagnation pressures. The subsonic jet (Fig. 3a) diverges quickly due to the Schlichting's similarity rule [10] and the aggressive shear mixing with ambient air does not allow sufficient vapor condensation. Thus, no Rayleigh scattering is detected for the subsonic jet, but the starry dots recorded in Fig. 3a show Mie scattering images from the airborne dust particles.

The nearly isentropic or perfect expansion (Fig. 3b) develops relatively weak condensation away from the nozzle exit. The slightly underexpanded sonic jet develops weak expansion fans (Fig. la), and the contact surface development will not be pronounced. The weak contact surface allows shear mixing of the jet with relatively warm ambient air, thus the vapor condensation will be enough to result in sufficient scattering.

When the jet is highly underexpanded (Figs. 3c and 3d), the vapor condensation amount noticeably increases, due to the additional temperature drop, via the successively

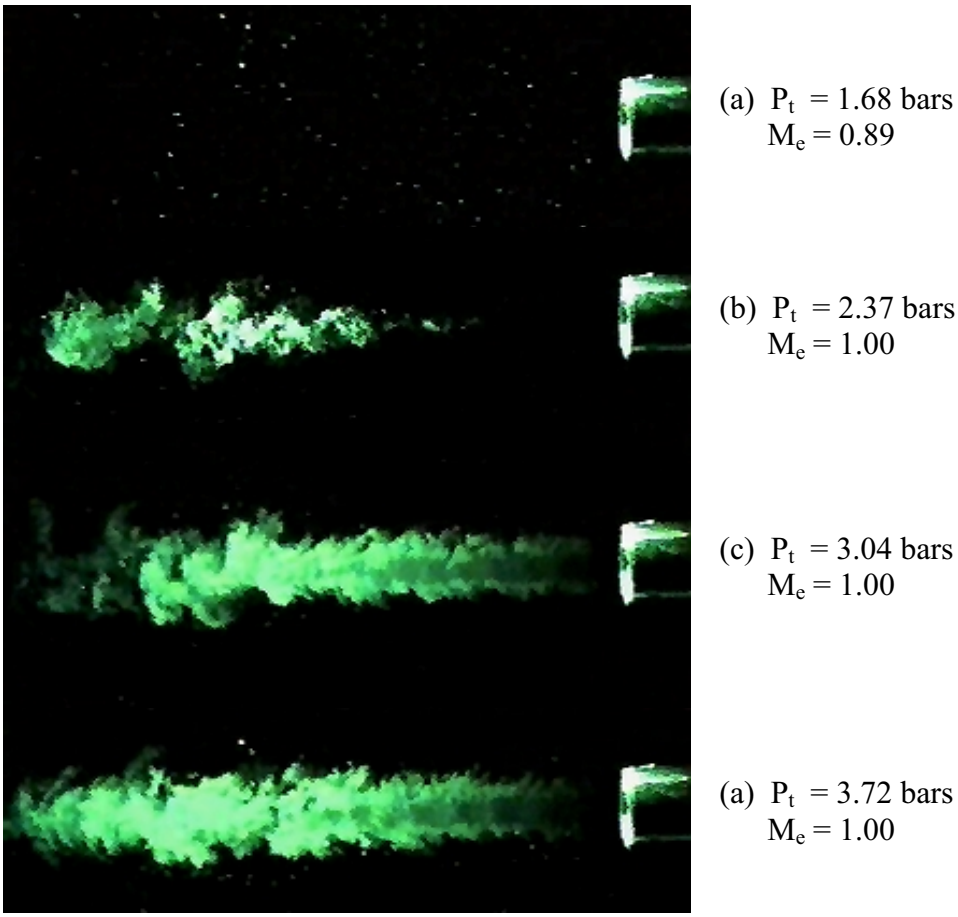

Fig. 3 Rayleigh scattering images of air jets exhausting from the SN type nozzle,

developing expansion fans (Fig. lb). The jet development is also narrowly confined within the contact surface formed by the reflection of expansion waves, and the vapor condensation will be more effective because shear mixing with warm ambient air is retarded. Another reason for the intense scattering is the increased number of condensed water molecules with increasing stagnation pressure.

Figure 4 shows the jet development from the CD type nozzle with 7.65 mm^2 throat area and 11.7 mm^2 exit area (the exit-to-throat area ratio $A/A^* = 1.53$). The subsonic jet (Fig. 4a) does not generate any visible condensation for the same reason as discussed for the SN type nozzle case above. The background dust images have been digitally eliminated. Figures 4b to 4d show the development and mixing of the overexpanded jet, while the nozzle exit Mach number M_e = 1.88 remains the same for all the three cases.

The stagnation pressures for Figs. 4b and 4c are ranged for the Mach disk [11], which is formed at or slightly downstream of the nozzle exit, respectively. The Mach disk, like normal shock waves but in a circular cross-sectional area, increases both flow pressure and temperature across it and the incoming supersonic flow decelerates to subsonic flow after the Mach disk. Figure 4b shows the subsonic jet emerging from the Mach disk located at the nozzle exit plane. The Mach disk in Fig. 4c is smaller in its cross-section, located slightly downstream of the nozzle exit; therefore, the image consists of a mixed jet of the central subsonic flow following the Mach disk and the concentric supersonic flow bypassing the Mach disk.

The jet in Fig. 4d repeatedly develops shock cell patterns alternating oblique shock waves and Prandtl-Meyer expansion fans (Fig. l b). While the CD type nozzle exit area is over 50% larger than the SN type nozzle, the former develops a narrower jet in comparison with the latter (Fig. 3d). This can be explained by the different initial jet formation, as illustrated in Fig. 1: the overexpanded jet contracts toward the centerline immediately after the CD type nozzle exit (Fig. lb), whereas the underexpanded jet expands outward as it emerges from the SN type nozzle (Fig. la). Also, the more definite development of the shock cell pattern of the CD type jet develops stronger contact surface and tends to confine the flow within the contact surface.

This develops the jet divergence more slowly compared with its counterpart for the SN type jet. On the other hand, the SN type jet diverges more rapidly along the axis because its contact surface is relatively weakly holding the jet.

Spray Angles and Development

Figure 5 shows Mie scattering spray images of the SN type nozzle for a constant water flow rate of $\dot{m}_L$ = 0.9 g/s, while the airflow rate increases with stagnation pressure. During the transition from subsonic (Fig. 5a), transonic (Fig. 5b) to underexpanded sonic (Fig. 5c) gas jets, the spray angle remains nearly unchanged and the spray development maintains the similarity. As discussed above, the weaker contact surface of the sonic jet is not able to hold the spray within it, and this is believed to be the reason why the sonic spray maintains the similarity as of the subsonic spray. The increased air-to-liquid ratio (ALR),

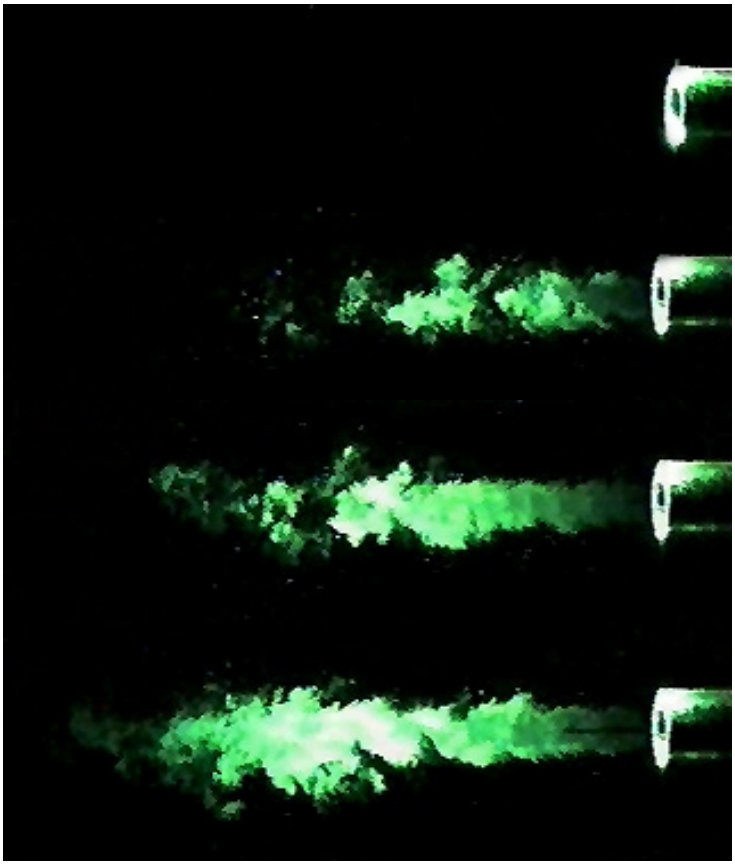

Fig. 4 Rayleigh Scattering images of air jets exhausting from the CD nozzle.

Fig.5 Mie scattering images of SN type nozzle sprays for constant liquid flow rate, $\dot{m}_L = 0.9 g/s$.

with increasing stagnation pressure, generates more dispersed sprays and less bright images due to the reduced Mie scattering intensity.

Figure 6 shows spray images under airblast by the CD type nozzle. The liquid injection rate is increased to $\dot{m}_L = 1.13 g/s$ in proportion to the increased air flow rate due to the 25% increase in the throat area compared with the SN type nozzle. The spray angle noticeably decreases during the transition from subsonic to supersonic gas jets with increasing ALR. The droplet concentration increases showing a brighter central area of intense scattering regions with increasing ALR.

Denser sprays increase the droplet concentration, and thereby enhance the probability of coalescence between droplets. This will contribute to the average droplet size increase compared with that of more dispersed sprays. The increased droplet concentration of the CD type sprays, because of their narrower spray development, will increase the droplet coalescence and produce slightly larger droplet mean diameters than their counterpart of the SN type sprays.

The difference in the spray angle, particularly for the high stagnation pressure range (e.g., Figs. Sc and 6c), may be partly explained by the different gas jet development between the two nozzles. The overexpanded flow from the CD type nozzle restricts the jet flow more strongly within its own contact surface and develops a relatively narrower air jet, while the SN type nozzle develops a sonic jet with a relatively weak contact surface.

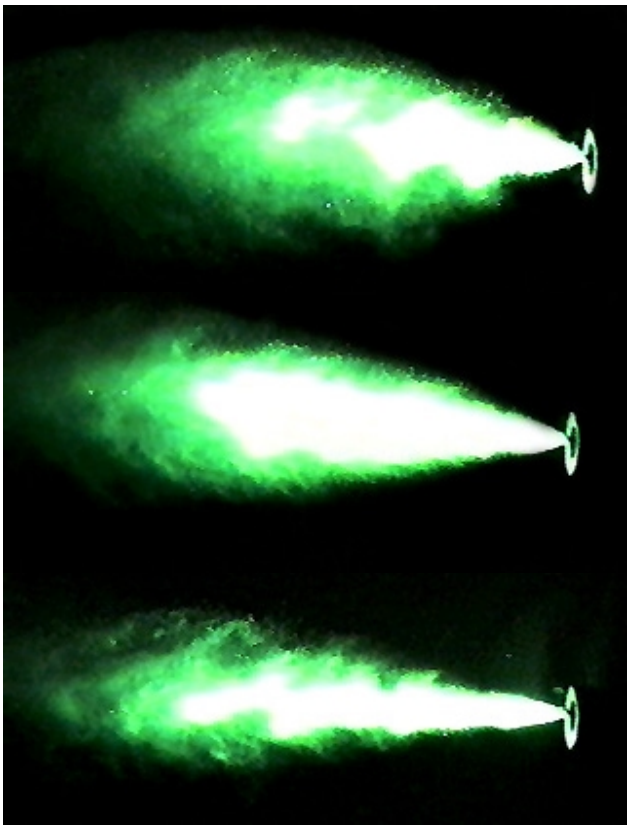

Fig. 6 Mie scattering images of the SN type nozzle sprays for constant liquid flow rate, $\dot{m}_L = 1.13g/s$.

The narrower air jet, with a strong contact surface from the CD type nozzle, tends to confine the spray development within a narrower angle as seen in Fig. 6c.

CONCLUSION

An overexpanded supersonic jet develops a stronger contact surface with a narrower initial jet cross-sectional area, compared with an underexpanded sonic jet. While the latter develops geometrically similar sprays to its subsonic counterpart, the former tends to restrict the spray within its contact surfaces, and, consequently, develops narrower sprays. The narrower spray contributes to the enhancement of the droplet coalescence and increases the spray drop SMDs more so than the relatively wider sprays from underexpanded sonic jets.

REFERENCES

1. J. A. Schetz, P. W. Hewitt, and M. Situ, Transverse Jet Breakup and Atomization with Rapid Vaporization Along the Trajectory, *AIAA J.*, vol. 23, no. 4, pp. 596-b03, 1985.
2. A. Unal, Liquid Breakup in Gas Atomization of Fine Aluminum Powders, *Metall. Trans. B,* vol. 20B, pp. 61-69, 1989.

3 K. D. Kihm and N. Chigier, Effect of Shock Waves on Liquid Atomization of a TwoDimensional Airblast Atomizer, *Atomization and Sprays,* vol. 1, pp. 113-136, 1991.
4. B. K. Park, J. S. Lee, and K. D. Kihm, Comparative Study of Twin-Fluid Atomization Using Sonic or Supersonic Gas Jets, *Atomization and Sprays,* vol.6, pp. 285-304, 1996.
5. E. Hecht, *Optics* (2nd ed.), Addison Wesley, Reading, Ch. 8, 1987.
6. P. Desevaux, J. P. Prenel, and G. Hostache, Flow Visualization Methods for Investigating an Induced Flow Ejector, J. Flow *Visualization and Image Processing, Vol.* 2, No. 1, pp. 6174, 1995.
7. D. A. Long, *Raman Spectroscopy,* McGraw-Hill, New York, Ch. 3, 1977.
8. T. K. Kim, Investigation of Sonic/Subsonic Air-Blast Atomization Using Rayleigh- and MieScattering Visualization Technique, M.S. thesis, Department of Mechanical Engineering, Texas A&M University, College Station, Texas, 1996.
9. C. F. Bohren and D. R. Huffman, *Absorption and Scattering of Light by Small Particles,* Wiley, New York, Ch. 4, 1983.
10. H. Schlichting, *Boundary Layer Theory* (6th ed.), McGraw-Hill, New York, Ch. XI, 1968.
11. J. E. A. John, *Gas Dynamics* (2nd ed.), Prentice-Hall, Englewood Cliffs, Ch. 7, 1984.